Journal of The Electrochemical Society, **146** (12) 4659-4665 (1999)
S0013-4651(99)04-011-2 CCC: $7.00 © The Electrochemical Society, Inc.

Bifurcation Analysis of Thermal Runaway in Microwave Heating of Ceramics

Nikunj Gupta, Vikas Midha, Vemuri Balakotaiah, and Demetre J. Economou*,z

Department of Chemical Engineering, University of Houston, Houston, Texas 77204-4792, USA

The steady-state behavior of a ceramic slab under microwave heating by transverse magnetic illumination is analyzed. Local bifurcation techniques are applied to a one-dimensional model to classify the region of parametric sensitivity (or thermal runaway). It is observed that for a certain set of parameters, there are periodically recurring ranges of slab thickness for which thermal runaway may be avoided. The runaway dependence on other parameters critical to the operation of the process is also studied. The results presented here may be used to prevent thermal runaway in microwave heating of ceramics.

Manuscript submitted April 5, 1999; revised manuscript received July 8, 1999.

Microwave heating has been applied in a variety of applications including sintering and joining of ceramics[1] and chemical vapor infiltration of fiber-reinforced ceramic composites.[2-5] One of the major hurdles currently faced in the application of microwave processing of ceramics is the occurrence of thermal runaway.[6] This phenomenon corresponds to a situation in which a small change in the design or operating variables (such as the thickness of the sample or microwave power) causes a rather large increase (of the order of several hundred degrees) in the temperature of the material being heated. Thermal runaway may also lead to melting of the ceramic material. It occurs due to the coupling of the thermal and electric fields and a positive feedback mechanism similar to that encountered in chemical reactors. Specifically, a small increase in temperature increases the dissipation rate (through the loss moduli which increases exponentially with temperature) and leads to a further increase in temperature. This leads to the familiar ignition and extinction phenomenon observed in chemical reactors and combustion. Under these conditions the steady-state temperature of the ceramic material is not a continuous function of the applied power.

Several efforts have been made to understand and quantify thermal stability of dielectric materials heated by microwave energy. These studies can be classified into three groups. The first group of models[7,8] assumes a uniform electric field and temperature distribution within the material. The second group[8,9] of models uses a constant electric field but includes spatial variations in temperature. The third group[10,11] of models assumes a low Biot number limit, and hence a uniform temperature inside the ceramic, but a spatially dependent electric field. Most of these studies analyzed the steady-state behavior of a ceramic material under microwave heating. They confirmed the existence of ignition and extinction phenomena as the microwave power is increased or decreased. Spotz *et al*.[8] showed the variation in the critical temperature (temperature at which ignition or runaway is first observed) with the temperature exponent of the loss moduli. The lumped (spatially uniform) models used in these studies are valid only for certain limiting cases and do not give a complete picture of runaway behavior.

In this work we discuss the steady-state behavior of a full one-dimensional model which accounts for spatial variation of both temperature and electric fields. We focus mainly on thermal runaway and how it depends on several important process parameters such as sample thickness, frequency of the microwaves, the loss modulus of the material, and the temperature sensitivity of the loss modulus. In the next section we present the mathematical model used for the analysis. Then we discuss briefly the mathematical (bifurcation) and numerical techniques used to analyze and classify the behavior of the steady-state model. Finally, we present the results and discuss some approaches to avoid thermal runaway during microwave heating of ceramic materials.

* Electrochemical Society Active Member.
z E-mail: economou@uh.edu

Mathematical Model

We assume that the sample thickness is much smaller compared to the lateral dimensions so that a one-dimensional model is a reasonable representation of the system. We assume that a plane time-harmonic electromagnetic wave of frequency ω impinges normally and the ceramic material is isotropic. A portion of the wave is scattered at the interface $x = 0$, a portion penetrates the slab and heats the material, and the remaining portion is transmitted through the other interface at $x = d$. The electric field and thermal energy balance for the ceramic slab are given by the following equations.[10]

Electric field equation.—

$$\frac{d^2U}{dx^2} + \bar{k}_1^2\left(1 + i\frac{\sigma_o(T)}{\omega\epsilon_1}\right)U = 0 \qquad 0 < x < d \qquad [1a]$$

In this equation $\bar{k}_1 = \omega/c\ (\epsilon_1/\epsilon_o)^{1/2}$, where ϵ_1 is the permittivity of the ceramic material, ϵ_o is the permittivity of free space, and $\sigma_o(T)$ is the relative loss modulus of the material. The boundary conditions at the two ends of the slab are given by

$$\frac{dU}{dx} + i\bar{k}U = 2i\bar{k}E_o \qquad \text{at } x = 0 \qquad [1b]$$

$$\frac{dU}{dx} - i\bar{k}U = 0 \qquad \text{at } x = d \qquad [1c]$$

where $\bar{k} = \omega/c$ and E_o is the electric field applied at the boundary $x = 0$.

Energy balance.—

$$\rho C_p\frac{\partial T}{\partial t} = K\frac{\partial^2 T}{\partial x^2} + \frac{1}{2}\sigma_o(T)|U|^2 \qquad 0 < x < d \qquad [2a]$$

At the boundaries of the slab, heat is lost by convection and radiation to the surroundings

$$K\frac{\partial T}{\partial x} = h(T - T_o) + \sigma e(T^4 - T_o^4) \qquad \text{at } x = 0 \qquad [2b]$$

$$-K\frac{\partial T}{\partial x} = h(T - T_o) + \sigma e(T^4 - T_o^4) \qquad \text{at } x = d \qquad [2c]$$

where K is the thermal conductivity of the material, h is the convective heat-transfer coefficient, σ is the Stefan-Boltzmann constant, and e is the emissivity of the material.

S0013-4651(99)04-011-2 CCC: $7.00

For materials such as Al_2O_3 and ZrO_2, for which thermal runaway is observed, the relative loss modulus increases exponentially with temperature and a relation of the form $\sigma_o(T) = b_1 e^{b_2 T}$ may be used, where b_1 and b_2 are constants determined experimentally.[8,12]

Defining dimensionless variables and parameters as

$$\xi = \frac{x}{d} \qquad u = \frac{U}{E_o} \qquad \theta = \frac{T - T_o}{T_o}$$

$$k = \bar{k}d \qquad \lambda = \frac{\bar{k}_1}{k} \qquad Bi = \frac{hd}{K} \qquad [3]$$

$$R = \frac{\sigma e T_o^3}{h} \qquad \nu = b_2 T_o \qquad \tan d_o = \frac{b_1 e^{b_2 T_o}}{\omega \epsilon_1}$$

and normalizing the applied power $p = 1/2\omega\epsilon_1 E_o^2$ by $p_c = KT_o/d^2$, the governing equations may be written as

Electric field equation.—

$$\frac{d^2u}{d\xi^2} + \lambda^2 k^2 (1 + i \tan d_o e^{\nu\theta}) u = 0 \qquad 0 < \xi < 1 \qquad [3a]$$

with boundary conditions

$$\frac{du}{d\xi} + iku = 2ik \qquad \text{at } \xi = 0 \qquad [3b]$$

$$\frac{du}{d\xi} - iku = 0 \qquad \text{at } \xi = 1 \qquad [3c]$$

Energy balance.—Since we consider only the steady-state behavior of the system, we drop the time derivative term in Eq. 2a. The dimensionless form of the energy balance is given by

$$\frac{d^2\theta}{d\xi^2} + \frac{p}{p_c} \tan d_o e^{\nu\theta} |u|^2 = 0 \qquad 0 < \xi < 1 \qquad [4a]$$

with boundary conditions

$$\frac{d\theta}{d\xi} = Bi\left\{\theta + R[(\theta + 1)^4 - 1]\right\} \qquad \text{at } \xi = 0 \qquad [4b]$$

$$-\frac{d\theta}{d\xi} = Bi\left\{\theta + R[(\theta + 1)^4 - 1]\right\} \qquad \text{at } \xi = 1 \qquad [4c]$$

Besides the applied microwave power p, other critical parameters that determine the qualitative behavior are the ambient loss modulus ($\tan d_o$), the temperature sensitivity coefficient (ν), and the dimensionless slab thickness (k).

The problem consists of one complex equation for the electric field (Eq. 3a) along with one real equation for temperature (Eq. 4a) to be solved simultaneously for the steady state. The complex electric field equation can be separated into two real equations, which leaves us with three simultaneous second-order coupled boundary value problems. We use the finite difference method to discretize these equations and solve the resulting algebraic equations numerically.

Bifurcation Analysis of the Steady-State Discretized Model and Computation of Singular Points

The discretized steady-state model consists of $N(=3n)$ equations for the temperature and for the real and complex electric field components at n nodal points. We are interested in determining how the number of solutions to this system of nonlinear algebraic equations changes as the parameters are varied.

Consider solving N nonlinear equations in N state variables $\mathbf{u}$, dependent on a set of m parameters $\mathbf{p}$

$$\mathbf{F}(\mathbf{u}, \mathbf{p}) = \mathbf{0} \qquad \mathbf{u} \epsilon R^N, \ \mathbf{p} \epsilon R^m \qquad [5]$$

Suppose that $\mathbf{u} = \mathbf{u}_0$ is a solution for $\mathbf{p} = \mathbf{p}_0$. Let

$$\mathbf{L} = D_u \mathbf{F}(\mathbf{u}_0, \mathbf{p}_0) = \frac{\partial F_i}{\partial u_j} \qquad i = 1,\ldots,N; \ j = 1,\ldots,N \qquad [6]$$

be the $N \times N$ Jacobian matrix. Expanding the vector function $\mathbf{F}$ in a Taylor's series around point $(\mathbf{u}_0, \mathbf{p}_0)$ gives

$$\mathbf{F}(\mathbf{u}, \mathbf{p}) = \mathbf{F}(\mathbf{u}_0, \mathbf{p}_0) + D_u \mathbf{F}(\mathbf{u}_0, \mathbf{p}_0)(\mathbf{u} - \mathbf{u}_0) + D_p \mathbf{F}(\mathbf{u}_0, \mathbf{p}_0)(\mathbf{p} - \mathbf{p}_0) + \text{h.o.t} \qquad [7]$$

(HOT stands for higher order terms.) Here $D_p \mathbf{F} = \partial F_i / \partial p_j$ is a $N \times M$ matrix. Using the fact that $\mathbf{F}(\mathbf{u}, \mathbf{p}) = \mathbf{F}(\mathbf{u}_0, \mathbf{p}_0) = 0$ at steady state and truncating the Taylor's series at the linear terms gives

$$\mathbf{L}(\mathbf{u} - \mathbf{u}_0) + D_p \mathbf{F}(\mathbf{u}_0, \mathbf{p}_0)(\mathbf{p} - \mathbf{p}_0) = 0 \qquad [8]$$

These linear equations describe how the solution varies for small changes in the parameter vector $\mathbf{p}$. If the matrix $\mathbf{L}$ is invertible we can express the new solution $\mathbf{u}$ in terms of $\mathbf{u}_0$ and the parameter vector $\mathbf{p}$ in the neighborhood of $\mathbf{p}_0$ as

$$\mathbf{u} = \mathbf{u}_0 - \mathbf{L}^{-1} D_p \mathbf{F}(\mathbf{u}_0, \mathbf{p}_0)(\mathbf{p} - \mathbf{p}_0) \qquad [9]$$

This operation results in a unique solution for $\mathbf{u}$, close to $\mathbf{u}_o$, as the parameters, $\mathbf{p}$, are varied. For the case when $\mathbf{L}$ is singular (or noninvertible) with a simple zero eigenvalue, it can be shown that either a new solution branch emerges from $\mathbf{u}_0$ or two solution branches merge.[13,14] These points are termed bifurcation or limit points. The parameter values at which bifurcation or limit points occur satisfy the following set of equations

$$\mathbf{F}(\mathbf{u}, \mathbf{p}) = 0 \qquad [10a]$$

$$\mathbf{L}\mathbf{y}_0 = 0 \qquad [10b]$$

$$\langle \mathbf{y}_0, \mathbf{y}_0 \rangle = 1 \qquad [10c]$$

($\langle \mathbf{y}_0, \mathbf{y}_0 \rangle$ implies the dot or inner product.) Equation 10c is a condition for nontriviality of the eigenvector $\mathbf{y}_0$. The above set of $2N + 1$ equations can be solved simultaneously for any one parameter (keeping other parameters fixed) at a point of bifurcation (or a limit point) and the vectors $\mathbf{u}$ and $\mathbf{y}_0$. Equivalently, we can plot a locus in a two-parameter space (which is known as the limit point locus or bifurcation set). When the parameters cross this set, the number of solutions of Eq. 5 changes. For the problem studied here the bifurcation set consists of two branches, *i.e.*, the ignition and extinction locus. The bifurcation set separates the parameter space into two regions corresponding to either one or three solutions.

Computation of the singular points.—We now illustrate the technique used to compute the limit points of the steady-state discretized model. The discretized model is given by Eq. 10a-c. These form a set of $2N + 1$ equations, which determines the $2N$ unknowns $(\mathbf{u}, \mathbf{y}_0)$ and one additional parameter in $\mathbf{p}$. The straightforward approach is to compute the function $\mathbf{F}$ and determine its Jacobian matrix, $\mathbf{L}$, numerically. Then the eigenvector $\mathbf{y}_0$ is evaluated and used in the defining conditions for the limit point. In order to reduce computing time and storage requirements we do not compute the Jacobian matrix explicitly but compute the product of $\mathbf{L}$ and $\mathbf{y}_0$ by using the definition

$$\mathbf{L}\mathbf{y}_0 = D_u \mathbf{F}(\mathbf{u}_0, \mathbf{p}_0)\mathbf{y}_0 = \left(\frac{\partial}{\partial s}\mathbf{F}(\mathbf{u}_0 + s\mathbf{y}_0, \mathbf{p}_0)\right) \quad \text{at } s = 0 \qquad [11]$$

Continuation of the singular points.—A pseudo-arc length continuation technique[15] is used to compute the limit point locus in a two-parameter space. If $\overline{\mathbf{X}}$ is a solution vector and p_i ($i = 1,2$) are the two parameters, the set of equations given is augmented by the single equation

$$s^2 - \left|\overline{\mathbf{X}} - \overline{\mathbf{X}}_0\right|^2 - \sum_{i=1}^{2} (p_i - p_{i,0}) = 0 \qquad [12]$$

S0013-4651(99)04-011-2 CCC: $7.00 © The Electrochemical Society, Inc.

where s is the step size and the subscript 0 denotes values at the previous step.

The continuation step size, s, may be adjusted depending on the sensitivity of parametric region. Beginning with an initial choice for s, a multiplicative factor determines the step size for the next step depending on the number of iteration steps in the actual continuation step. In this work, the step-size control was adjusted such that the optimum number of iterations remain between two and five at every continuation step.

Solution of the set of nonlinear algebraic equations.—The set of algebraic equations, which is the result of discretization, may be written as

$$\mathbf{G}(\mathbf{X}) = \begin{pmatrix} \mathbf{F}(\mathbf{u},\mathbf{p}) \\ \mathbf{L}\mathbf{y}_0 \\ \langle \mathbf{y}_0, \mathbf{y}_0 \rangle - 1 \\ s^2 - \left|\overline{\mathbf{X}} - \overline{\mathbf{X}_0}\right|^2 - \sum_{i=1}^{2} (p_i - p_{i,0}) = 0 \end{pmatrix} = 0 \quad [13]$$

$$(\overline{\mathbf{X}}) = (\mathbf{u}, \mathbf{y}_0)^T, \quad \mathbf{X} = (\overline{\mathbf{X}}, p_1, p_2)^T \quad [14]$$

The standard Newton-Raphson method was applied to solve this set of nonlinear algebraic equations. The final vector equation $\mathbf{G}(\mathbf{X}) = 0$ consists of $2N + 2$ simultaneous scalar equations. At every Newton-Raphson iteration the Jacobian matrix $\mathbf{J}$ and the inverse matrix are numerically computed. The scheme converged for reasonably good initial guesses for the solution vector $\mathbf{X}$.

Results

We first illustrate results for a slab being heated in a microwave field with a gradual increase in the applied power starting at ambient temperature ($T = T_o$). As the power is increased slowly, the temperature of the ceramic also increases slowly, but at a critical value of the power there is a sudden jump in the temperature to a very high value, to the so-called ignited state. The temperature on this ignited branch could be in the range where the ceramic can melt down. Further increase in the applied power leads to a gradual increase in temperature. Similarly, if initially the state of the ceramic is on the high-temperature branch and the applied power is gradually decreased, the temperature of the ceramic decreases gradually until a certain critical value at which a sudden and sharp decrease occurs. When the microwave power is below this extinction limit, the ceramic is in the low-temperature (quenched) branch. Thus, the steady-state curve describing the center-line temperature exhibits hysteresis with two stable states (and one unstable state) when the applied power is between the ignition and extinction limits.

Figure 1 illustrates the above-described typical S-shaped steady-state behavior for a ceramic slab under microwave heating for d = 4.0 cm and other parameter values given in Table I. Such steady-state behavior has been reported by numerous authors.[8,10,11] Points marked (1) and (2) are the ignition and extinction point, respectively. They are characterized by the linearized steady-state system having a zero eigenvalue. Physical reasoning or stability analysis may be used to show that the middle steady-state branch between points (1) and (2) is unstable. Note that the power given in Fig. 1 is the applied power (P = 1/2 $WE_1E_o^2$) not the power dissipated in the ceramic (see also Fig. 13).

In Fig. 2 and 3 the square of the magnitude of the electric field and the temperature profiles are shown at the three different locations on the S-shaped curve noted in Fig. 1. It is observed that the electric field experiences spatially undamped oscillations at low temperatures which decay exponentially as the temperature is increased. Finally, at high enough temperatures, the electric field shows a simple exponential decay with a maximum at the surface. The temperature profile inside the ceramic (Fig. 3) is symmetric and displays a maximum near the center at low temperatures. However, the temperature profile becomes asymmetric and the maximum shifts toward the surface with increasing temperature. The maximum temperature never reaches the surface ($x = 0$) due to heat losses from the surface. These transitions in temperature and electric field profiles occur due to the exponential increase in the loss moduli (tan $d_o e^{\nu\theta}$) with temperature.

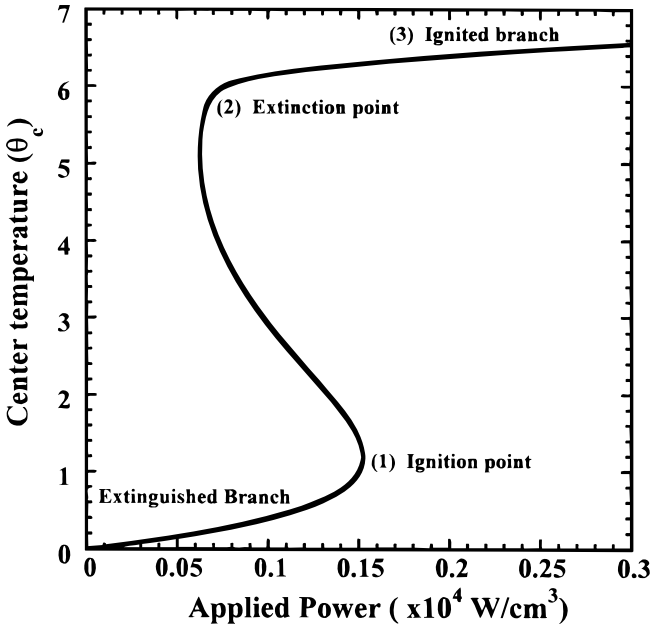

Figure 1. Simple S-shaped steady-state bifurcation diagram for ceramic slab (d = 4.0 cm). Other parameter values as in Table I.

Figure 4 illustrates how the ignition and extinction points move in the parameter space of microwave power and slab thickness (a bifurcation set). It is observed that the microwave power at which ignition and extinction occur oscillates with the slab thickness. Such peculiar behavior has not been reported for a physical system and can be attributed to the oscillations of the electric field inside the ceramic. It is also seen that the oscillations in the limit point (ignition and extinction) locus show an exponential decay with slab thickness, which can be attributed to the exponential decay of the electric field with thickness. An interesting observation from this bifurcation set is that as one goes toward larger slab thickness the oscillating ignition and extinction points merge (at a so-called hysteresis point) leading to formation of segregated loops (not shown in Fig. 4). The physical interpretation of this result is that there are "windows" in thickness where the bifurcation diagram of the center temperature *vs.* power is a single valued curve (with no ignition and extinction points), and no runaway occurs for any value of microwave power. For the parameter values we have chosen, this behavior seems to occur for thicknesses more than 12 cm. Later on we show that this behavior can occur for smaller slab thicknesses if we increase the microwave frequency or ceramic permittivity. Figure 5 gives a few representative bifurcation diagrams with

Table I. Base case parameter values used in calculations.

Ambient temperature	T_o (K)	300
Heat-transfer coefficient	h (W/m^2 K)	170
Thermal conductivity	K (W/m K)	10
Relative permittivity	ϵ_1/ϵ_o	10
Emissivity	e	0.7
Frequency	f (GHz)	2.45
Loss moduli (at T_o)	tan d_o	0.0012
Temperature exponent of loss moduli	ν	1.0

S0013-4651(99)04-011-2 CCC: $7.00

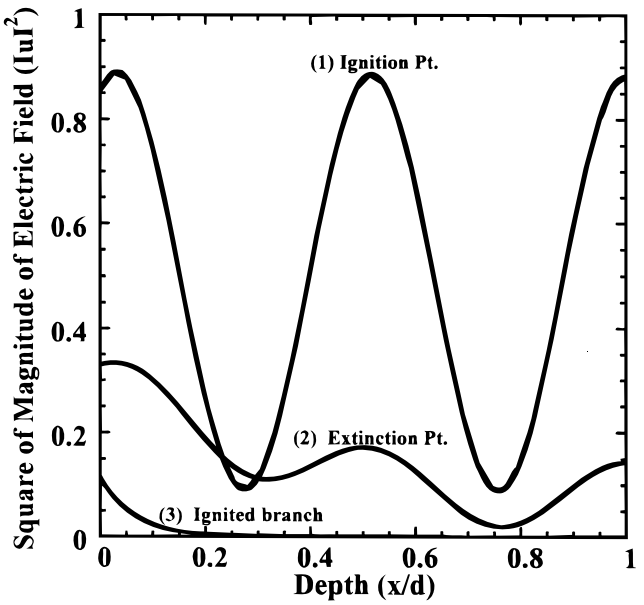

Figure 2. Electric field profiles inside the slab at the three different locations noted in Fig. 1.

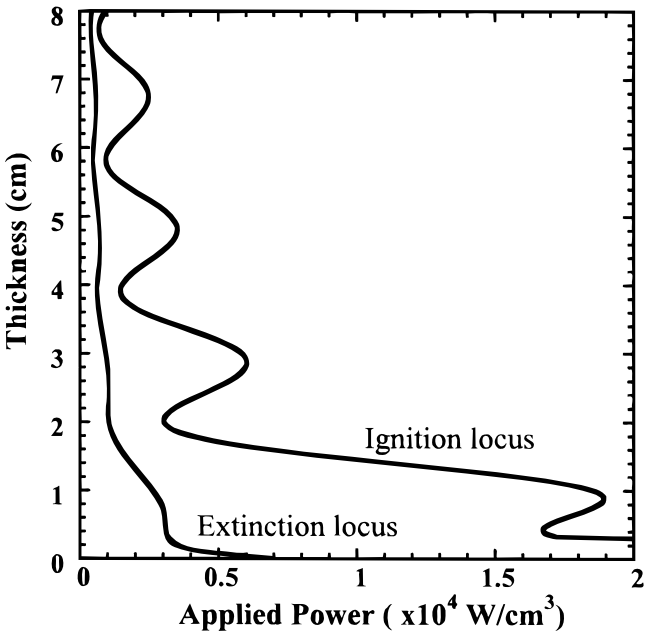

Figure 4. Bifurcation set in the parameter space of applied power and slab thickness. The two different curves correspond to the ignition and extinction locus. Other parameter values as in Table I.

microwave power being the operating (bifurcation) parameter. It is clearly seen in Fig. 4 that the range of power values for which we have multiplicity (difference between ignition and extinction points) grows and shrinks (*i.e.*, oscillates) as we change the thickness, but the oscillation amplitude shows an exponential decay with increasing thickness. Further interpretation of the behavior in Fig. 4 and 5 is shown in the bifurcation diagrams of Fig. 6 and 7 where we have taken the slab thickness as the operating parameter keeping the microwave power constant. These figures show that there is a range of thickness for which there exist steady-state multiplicities (more than one temperature for the same thickness) interspersed within a range of thickness for which a single steady state exists for a given microwave power. For ceramic sintering one may desire to operate at an intermediate temperature, not on the ignited branch, to avoid runaway. In such a case one may want to operate in a regime where there is no multiplicity for a given power so that one is not trapped in the lower (extinguished) temperature branch or does not jump to the very high temperature ignited branch.

Figure 8 gives another bifurcation set in the parameter space of ambient loss modulus (tan d_o) and microwave power. This plot was made for a slab thickness of 1 cm. It is observed that the two limit points merge (at a hysteresis point) as tan d_o increases. This implies that if we go in the direction perpendicular to the plane in Fig. 4 (in the parameter space of tan d_o), the oscillating loops seen in Fig. 4 shrink and finally disappear with increasing tan d_o, putting an end to runaway behavior. Thus, materials having higher loss moduli at

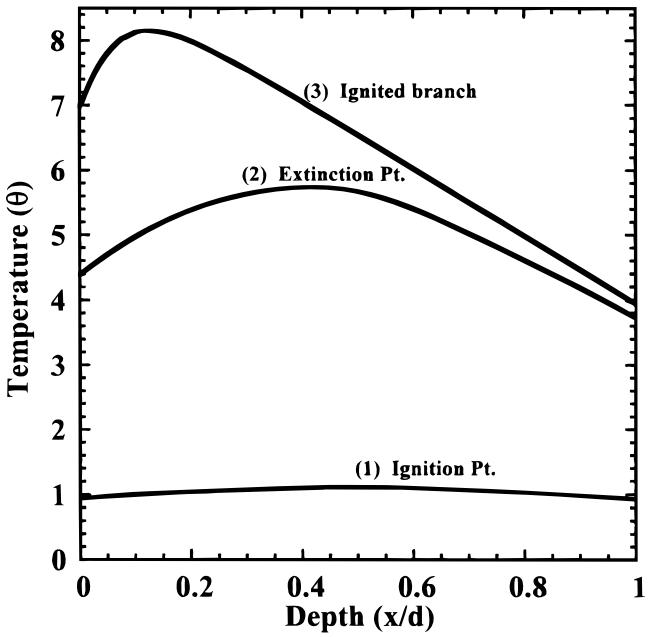

Figure 3. Temperature profiles inside the slab at three different locations noted in Fig 1.

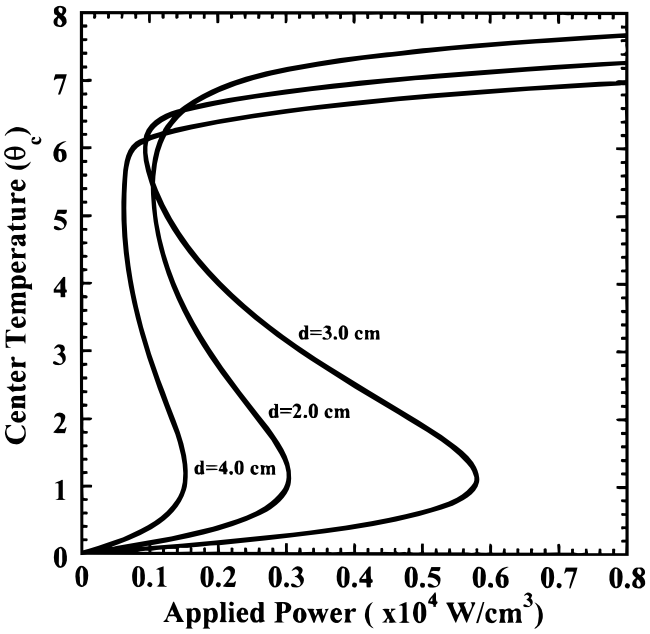

Figure 5. Steady-state bifurcation diagrams demonstrating the growing and shrinking of multiplicity in Fig 4.

S0013-4651(99)04-011-2 CCC: $7.00

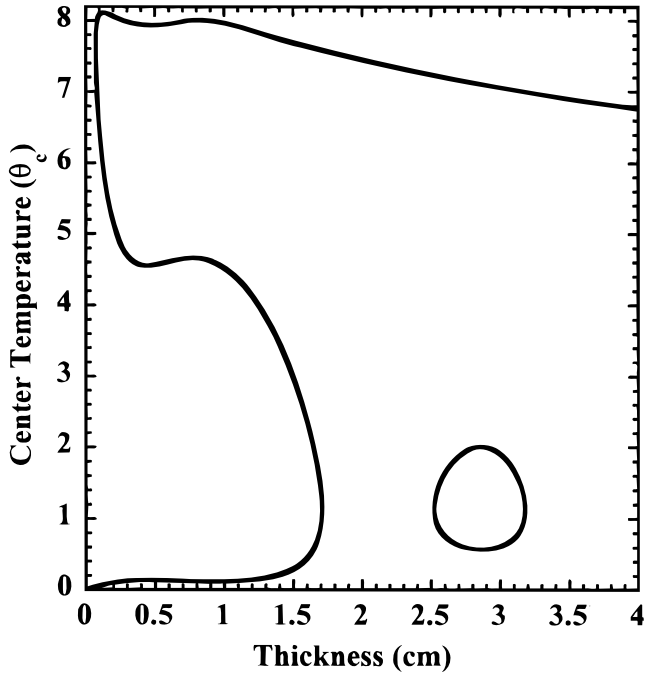

Figure 6. Steady-state bifurcation diagram using thickness as the bifurcation parameter demonstrating multiplicity and isolated solution branches (p = 5 kW/cm^3, other parameter values as in Table I).

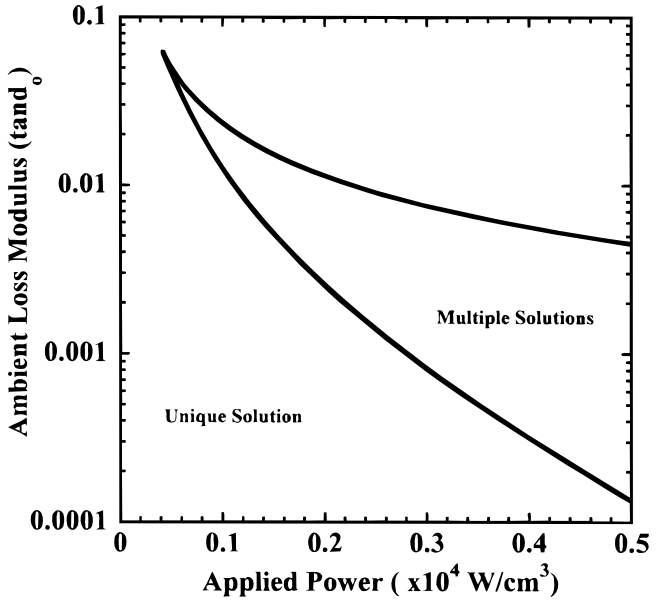

Figure 8. Bifurcation set in (tan d_o, p) space showing the merger of ignition and extinction points at higher values of tan d_o (d = 1.0 cm, other parameter values as in Table I).

ambient conditions have lesser chances of "running away" upon microwave heating. Another interpretation of this result would be to operate at elevated temperatures, increasing the loss modulus and averting runaway.

We now discuss how other relevant parameters affect the bifurcation behavior. An important parameter is the microwave frequency, which may range from 2.45 to 24.5 GHz under normal sintering conditions. The most commonly used frequency, though, is 2.45 GHz at which all the previous analysis was done. If one doubles the microwave frequency (f = 4.9 GHz) one sees a qualitatively similar bifurcation set (compare Fig. 9 to Fig. 4). Note that by doubling both the thickness and the microwave power in Fig. 9 one retraces Fig. 4 with minor changes. Thus, doubling the frequency rescales the problem. Also, it should be mentioned that by operating at higher frequency we can achieve the advantage of operating at larger thickness, thus availing the "windows" in thickness for which there is no runaway even for small slab thickness. Increase in permittivity has qualitatively the same effect as increase in frequency. Figure 10 gives a bifurcation set for a relative permittivity (ϵ_1/ϵ_o) of 60, keeping all other parameters as shown in Table I. It is evident that there are windows starting near thicknesses of 2.4, 3.2, 4.0, 4.8,

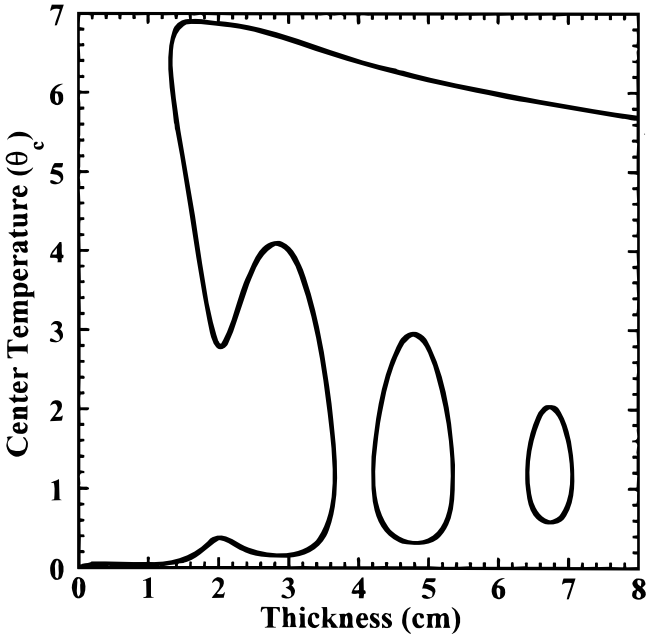

Figure 7. Steady-state bifurcation diagram using thickness as the bifurcation parameter demonstrating formation of new isolated solution branches (p = 2.5 kW/cm^3, other parameter values as in Table I).

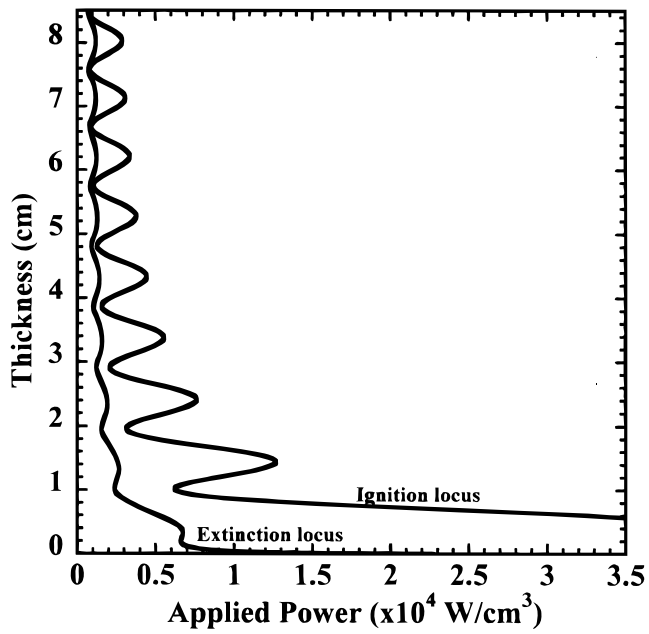

Figure 9. Bifurcation set in (d, p) space for f = 4.9 GHz. Doubling the frequency just rescales Fig. 4. Other parameter values as in Table I.

S0013-4651(99)04-011-2 CCC: $7.00

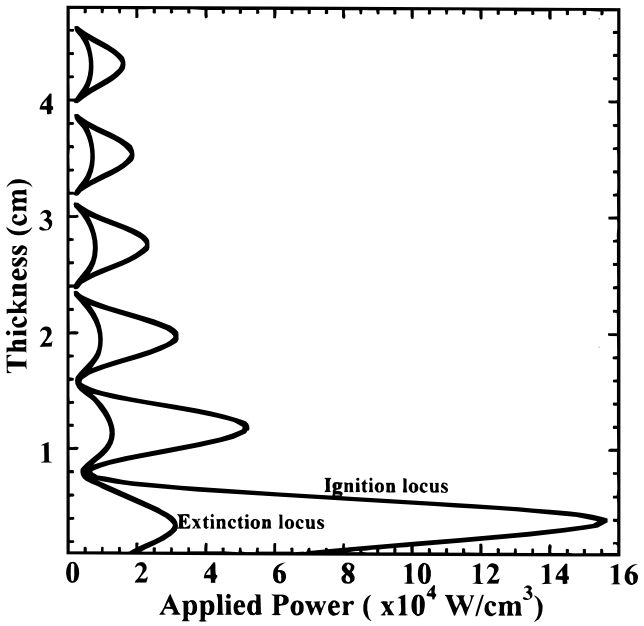

Figure 10. Bifurcation set in (d, p) space for $\epsilon_1/\epsilon_0 = 60$. Increasing permittivity moves "windows" of uniqueness toward smaller slab thickness. Other parameter values as in Table I.

.....cm, and these windows give more flexibility to operate while avoiding runaway. One such window is demonstrated in Fig. 11 which shows bifurcation diagrams where we have no multiplicity for a specific thickness ($d = 3.9$ cm) bracketed on either side by a multiple solution regime. A case without multiplicity is ideal in the sense that the desired temperature of the ceramic can be set uniquely by a microwave power setting.

It should be noted that the system can be sensitive even when the bifurcation diagram is single valued. For example, we see from Fig. 11 that when $d = 3.9$ cm there is a unique center temperature for any applied power. However, when p is close to 0.2×10^4 W/cm^3, the center temperature is sensitive to changes in p. Thus, while sudden jumps are not present in the unique solution region, the system can still exhibit "parametric sensitivity," where small changes in one of the operating variables (*e.g.*, power) result in large variation in the temperature.

The complementary effect of permittivity and frequency can be explained by the wavenumber $\bar{k}_1 (= 2\pi f/c(\epsilon_1/\epsilon_0)^{1/2})$. The inverse of this wavenumber defines the length scale of the electric field oscillations. The oscillations appearing in the bifurcation set have wavelength $C/\bar{k}_1$, where C is a constant. Thus, a relative change in operating frequency $\Delta f/f$ has a similar effect as a relative change in permittivity $\Delta\epsilon_1/\epsilon_1 = (\Delta f/f)^2$.

Further insight into the features presented may be provided by analyzing the same model with a constant loss modulus ($\nu = 0$). This would decouple the electric field equations, which are now linear and can be solved explicitly. Substitution of $u(\xi)$ in the energy balance Eq. 4a and integration gives a unique temperature profile. Thus, there will always be a unique solution when $\nu = 0$. For this case we plot the center temperature (Fig. 12) and power deposition (Fig. 13) variation with thickness. It can be seen that both oscillate with thickness. Also, the length scale of these oscillations (wavelength) is the same as the one in the bifurcation set, further corroborating the phenomenon described previously.

Finally, we note that for any small but nonzero value of ν, the boundary value problem defined by Eq. 3a-c and 4a-c has multiple solutions (for some range of other parameters). As ν is varied, the qualitative features remain the same but move to a different range in the parameter space. For example, the temperature of the ignition point may be approximated by $\theta_i \approx 1/\nu$. Thus, the temperature sensitivity parameter (ν) determines the ignition and extinction temperatures and hence strongly influences the runaway behavior.

Summary

In this work we have analyzed and classified the thermal behavior of a ceramic slab under microwave heating. Thermal runaway can occur due to a feedback mechanism whereby the ability of the material to absorb microwave energy (the loss modulus) increases as the temperature increases. Such thermal runaway can lead to complete meltdown of the material. Bifurcation theory was used to determine the region of thermal runaway and how it is influenced by important variables and parameters such as the microwave power, ceramic permittivity, relative loss modulus, microwave frequency, and slab thick-

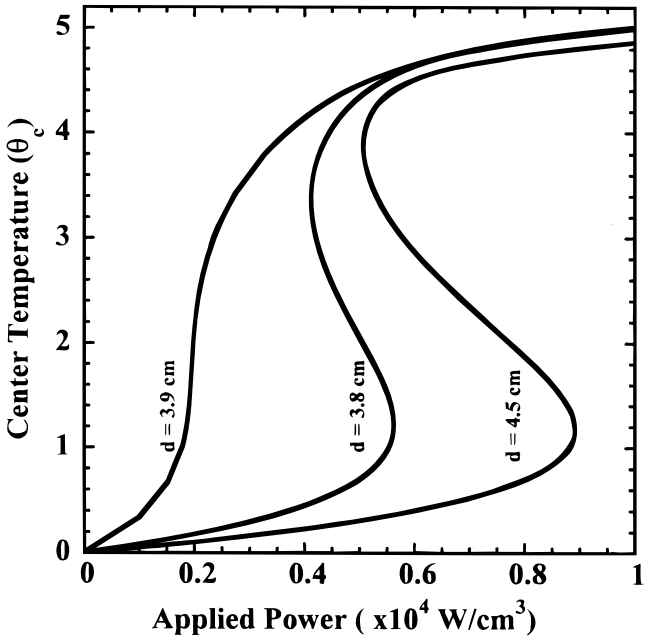

Figure 11. Steady-state bifurcation diagrams showing uniqueness (for $d = 3.9$ cm) of solution corresponding to "window" in Fig. 10.

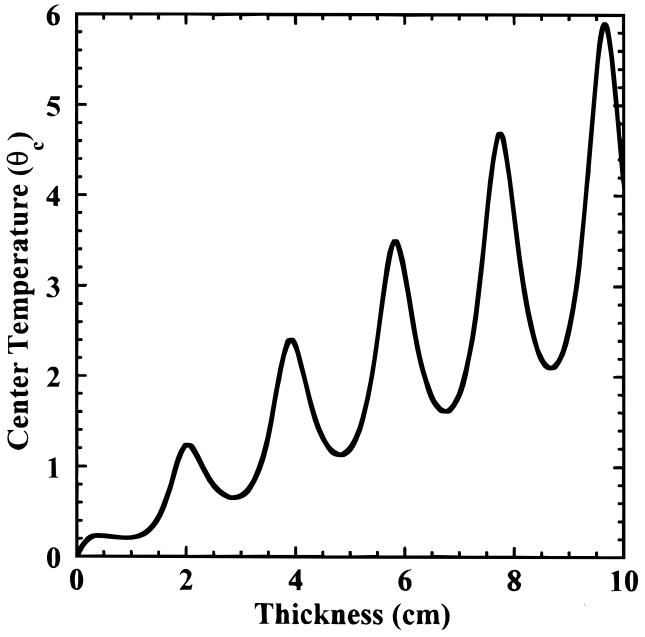

Figure 12. The "unique" temperature ($\nu = 0$) inside the ceramic oscillates as slab thickness is changed for a given microwave power ($p = 10$ kW/cm^3, other parameter values as in Table I).

S0013-4651(99)04-011-2 CCC: $7.00

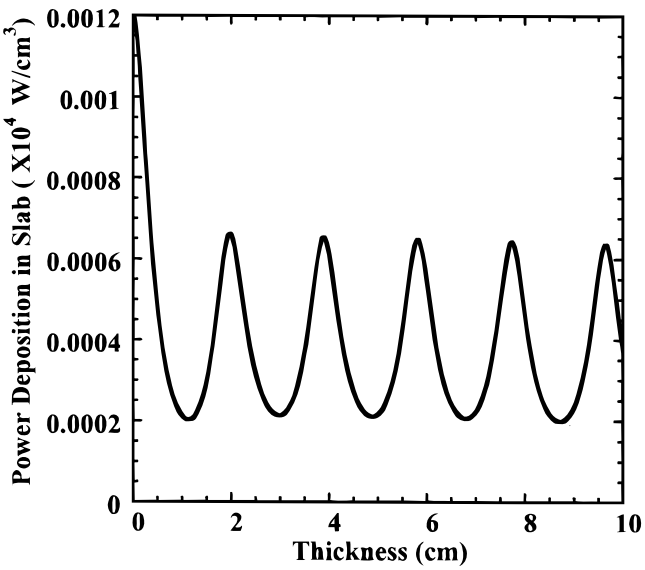

Figure 13. The "unique" power deposition ($\nu = 0$) inside the ceramic oscillates as slab thickness is changed for a given microwave power (p = 10 kW/cm^3, other parameter values as in Table I).

ness. It was found that for a certain set of parameter values which are within the range of practical systems, there are periodically recurring ranges of slab thickness for which thermal runaway may be avoided. Also, one can select operating parameters so as to suppress multiple solutions for the microwave-heated ceramic material. In such cases, the temperature of the ceramic is a unique function of the power absorbed by the ceramic, and thermal runaway does not occur as that power is increased. The one-dimensional model analyzed here provides much better insight into the behavior of the slab under microwave heating as compared to the lumped model used previously by several authors. The lumped model is an approximation to the actual process only in the limiting case of very small (and perhaps unrealistic) values of slab thickness. Finally, it should be pointed out that the analysis and techniques presented here may be used to analyze more complicated models (*e.g.*, two- and three-dimensional models) and the behavior of nonisotropic materials.

List of Symbols

Bi	Biot number
c	velocity of light, m/s
C_p	specific heat capacity of the ceramic
d	slab thickness, m
e	emissivity
E_o	applied electric field, V/m
h	ambient heat-transfer coefficient, W/(m^2 K)
$\bar{k}$	wavenumber of the incident microwave, m^{-1}
$\bar{k}_1$	wavenumber inside the ceramic, m^{-1}
K	thermal conductivity, W/(m K)
p	applied microwave power, W/m^3
T	temperature, K
U	electric field in the ceramic, V/m

Greek

ϵ_o	permittivity of free space, F/m
ϵ_1	permittivity of the ceramic, F/m
θ	dimensionless temperature
ν	temperature sensitivity of loss moduli
ξ	dimensionless depth inside the ceramic
ρ	density of the ceramic, kg/m^3
σ	Stefan-Boltzmann constant, W/(m^2 K^4)
σ_o	relative loss modulus of the ceramic
ω ($= 2\pi f$)	wave frequency, s^{-1}

Acknowledgments

This work was supported in part by the Energy Laboratory at the University of Houston.

References

1. W. D. Kingery, H. K. Bowen, and D. R. Uhlman, *Introduction to Ceramics*, John Wiley, New York (1976).
2. Deepak and J. W. Evans, *J. Am. Ceram. Soc.*, **76**, 1915 (1993).
3. Deepak and J. W. Evans, *J. Am. Ceram. Soc.*, **76**, 1924 (1993).
4. V. Midha and D. J. Economou, *J. Electrochem. Soc.*, **144**, 4026 (1997).
5. V. Midha and D. J. Economou, *J. Electrochem. Soc.*, **145**, 3569 (1998).
6. W. H. Sutton, *Am. Ceram. Soc. Bull.*, **68**, 376 (1989).
7. G. A. Kriegsmann, *Ceram. Trans.*, **59**, 269 (1995).
8. M. S. Spotz, D. J. Skamser, and L. D. Johnson, *J. Am. Ceram. Soc.*, **78**, 1041 (1995).
9. G. A. Kriegsmann and P. Varatharajah, *Ceram. Trans.*, **36**, 221 (1993).
10. G. A. Kriegsmann, *J. Appl. Phys.*, **71**, 1960 (1991).
11. C. A. Vriezinga, *J. Appl. Phys.*, **83**, 438 (1998).
12. S. Al-Asafi and D. E. Clark, *Mater. Res. Soc. Symp. Proc.*, **269**, 335 (1992).
13. M. Golubitsky and D. G. Schaeffer, *Singularities and Groups in Bifurcation Theory*, Vol. 1, Springer-Verlag, New York (1985).
14. V. Balakotaiah, D. Luss, and B. L. Keyfitz, *Chem. Eng. Commun.*, **36**, 121 (1985).
15. H. B. Keller, *Applications of Bifurcation Theory*, P. H. Rabinowitz, Editor, pp. 159-385, Academic Press, New York (1977).